Article

Study of the Effect of Adding Nb$_2$O$_5$ on Calcium Titanate-Based Ferroelectric Ceramics

Maxim V. Zdorovets [1,2], Gulnaz Zh. Moldabayeva [3,*], Inesh Z. Zhumatayeva [1], Daryn B. Borgekov [1,2], Rafael I. Shakirzyanov [1] and Artem L. Kozlovskiy [1,2]

1   Engineering Profile Laboratory, L.N. Gumilyov Eurasian National University, Satpayev St.,
    Nur-Sultan 010008, Kazakhstan; zhumatayeva@enu.kz (I.Z.Z.); borgekov@inp.kz (D.B.B.);
    shakirzyanov@enu.kz (R.I.S.); kozlovskiy.a@inp.kz (A.L.K.)
2   Laboratory of Solid State Physics, The Institute of Nuclear Physics, Ibragimov St., Almaty 050032, Kazakhstan
3   Department Petroleum Engineering, Satbayev University, Almaty 050013, Kazakhstan
*   Correspondence: g.moldabayeva@satbayev.university

Abstract: This paper considers the effect of adding niobium oxide (Nb$_2$O$_5$) to ferroelectric ceramics based on calcium titanate (CaTiO$_3$), and establishes a connection between the observed alterations in strength and dielectric properties and the variation in the Nb$_2$O$_5$ dopant concentration in the ceramics' composition. The method of mechanochemical solid-phase synthesis was used as the main method for obtaining the ceramics, followed by thermal sintering under specified conditions in order to form a stable phase composition of the ceramics, and to initialize phase transformations in the composition. Based on the assessment of the phase composition of the resulting ceramics, it was determined that a growth in the Nb$_2$O$_5$ dopant concentration beyond 0.10 mol results in the formation of an orthorhombic-phase CaNb$_2$O$_4$ of the Pbcm(57) spatial system, the weight contribution of which grows. A growth in the Nb$_2$O$_5$ additive concentration results in the formation of two-phase ceramics, the formation of which allows for an enhancement in the mechanical strength of ceramics and resistance to external influences. During the study of the dependence of the strength properties on the dopant concentration alteration, a three-stage change in hardness and crack resistance was established, regarding both structural ordering and phase transformations. The measurement of dielectric characteristics showed the direct dependence of dielectric losses and the dielectric constant on the phase composition of ceramics.

Keywords: ferroelectrics; doping; calcium titanate; ceramics; strength properties

1. Introduction

Interest in ferroelectric ceramics is growing exponentially due to the large number of different practical applications of these types of ceramics, both in energy (the basis for creating fuel cells, batteries or capacitors), sensors (to create highly sensitive sensors), and as photocatalysts or adsorbents for the decomposition of organic dyes or purification of aqueous media [1–3]. At the same time, the number of scientific publications covering such studies is increasing annually. First of all, this is due to a wide diversity of possibilities for varying the composition of ferroelectric ceramics, as well as methods for their production or modification [4–8]. Also, much attention has been paid to fundamental research aimed at the comprehensive study of the connection between the structural, optical, dielectric, and strength properties of ceramics obtained by various methods [9,10]. Much attention in the last few years has been paid to the research direction associated with the possibility of the directional modification of ferroelectric perovskite or perovskite-like ceramics of the ABO$_3$ type, the main purpose of which is to increase their resistance to external influences during operation, since it is the stability and the preservation of stability of properties as a result of external influences that makes it possible to determine the limits of applicability of these ceramics [11–15].

The most favorable direction of the application of ferroelectric ceramics is their use as anode materials for solid oxide fuel cells, interest in which is primarily due to the possibility of increasing the share of alternative energy sources in the energy sector, as well as the possibility of abandoning traditional energy sources, primarily from hydrocarbons [16,17]. Interest in ferroelectrics of the perovskite type ABO_3, which are based on oxide compounds of rare earth and alkali metals, as well as transition metal oxides, is primarily due to their dielectric and electrocatalytic properties [18,19]. Also, the choice of ferroelectric ceramics when used as anode materials is due to their thermodynamic stability and resistance to external high-temperature influences, which leads to the possibility of using them as the most promising alternative materials to classical Ni/NiO + YSZ compounds [20,21], used as anode materials, but at the same time, they have a number of disadvantages, the elimination of which has been planned through a transition to perovskite-like ferroelectrics of the ABO_3 type [22,23]. Among the varieties of perovskite ferroelectrics of the ABO_3 type, it is worth highlighting ceramics based on calcium ($CaTiO_3$), barium ($BaTiO_3$), and strontium ($SrTiO_3$) titanates, which have a number of unique properties, such as a high dielectric constant, thermal stability, and spontaneous polarization, which makes them the most common materials for use as a basis for microelectronic devices, including the creation of anode materials for solid oxide fuel cells [24–27]. Moreover, considerable focus has been directed not just toward the techniques for producing these ceramics but also toward exploring strategies for altering them through doping with various compounds (usually Nd_2O_3, Nb_2O_5, Y_2O_3, CeO_2, La_2O_3), the use of which makes it possible to create ceramics with improved properties, and to enhance their resistance both to external influences and to long-term thermal heating during operation [28–32].

The purpose of this paper is to study the relationship between the structural, mechanical, and dielectric characteristics of ferroelectric ceramics based on calcium titanate doped with Nb_2O_5 at various concentrations. Solid-phase mechanochemical synthesis in combination with thermal annealing of the obtained samples was used as a preparation method in order to initialize the processes of phase transformations. The choice of the method for obtaining ceramics is based on the simplicity of obtaining, as well as the possibility of scaling, this production technology on an industrial scale while maintaining all the properties of the synthesized ceramics. In turn, the choice of Nb_2O_5 as a dopant for modifying ceramics is due to the possibility of changing their dielectric characteristics, which, in turn, allows using them as anode materials, as well as to increase the resistance to external influences (mechanical and thermal), including the improvement in thermal stability because of the substitution effect or the formation of impurity phases.

2. Materials and Methods of Research

As a method for obtaining ferroelectric ceramics based on calcium titanate doped with niobium oxide (Nb_2O_5), the method of solid-phase synthesis based on the mechanochemical milling of the initial components in a specified stoichiometric ratio was used. The process of mechanochemical synthesis involves the combination of mechanical action and chemical reactions to obtain desired composites or ceramics. For grinding the samples using mechanochemical synthesis, a PULVERISETTE 6 classic line planetary mill (Fritsch, Berlin, Germany) was used. For grinding, the samples were placed in a mixing beaker with a volume of 80 mL in a ratio of 1:3 to grinding balls with a diameter of 10 mm (number of 20 pcs.). A grinding speed of 400 rpm was chosen to avoid the cold mechanical welding of the specimens on the walls of the tungsten carbide (WC) cup.

Thermal sintering for the purpose of initializing the processes of phase transformations and structural ordering depending on the concentration of the Nb_2O_5 dopant was carried out in an oxygen-containing environment in an SNOL muffle furnace (SNOL, Utena, Lithuania). Sintering was carried out at a temperature of 1200 °C for 8 h. Heating was carried out at a rate of 20 °C/min; when the set temperature was reached, the samples were kept for a certain time, followed by cooling for 24 h without removing the samples from the oven.

As a result of using the method of solid-phase synthesis, it is possible to obtain ferroelectric ceramics based on calcium titanate doped with niobium oxide. This material has ferroelectric properties, which means that it is capable of exhibiting electrical polarization in the presence of mechanical stress.

To measure the resistance to external influences, as well as the dielectric properties, the obtained samples were pressed at a maximum pressure of 200 MPa into tablets 12.1 mm in diameter and 1 mm thick using a binder from an aqueous solution of polyvinyl alcohol. Next, the pellets were annealed at 1000 °C to remove the binder.

The morphological characteristics of the synthesized ceramics contingent on the variation of the Nb_2O_5 dopant component were examined by means of scanning electron microscopy. A Hitachi TM3030 microscope (Hitachi, Tokyo, Japan) was used to obtain images. The images were taken in the lower secondary electron (LEI) mode with the possibility of obtaining high-resolution contrast images showing the grain morphology of the synthesized ceramics.

The study of the phase composition, as well as the formation of the crystal structure of ferroelectric ceramics, was carried out using the X-ray phase analysis method implemented using a D8 Advance ECO powder X-ray diffractometer (Bruker, Berlin, Germany). The diffractograms used for interpretation and full profile analysis were obtained in the Bragg–Brentano geometry in the angular range of $2\theta = 20$–$100°$, with a step of $0.03°$. The weight contributions of various phases were estimated by refining the intensities and weight areas of the reflection characteristic of the established phases. The structural ordering degree, which reflects the structural order and perfection of the crystal lattice, was determined by calculating the ratio of the areas of reflections and background radiation. To assess the structural parameters and the degree of structural ordering, the full-profile analysis method was used. The lattice parameters for each phase were determined using DiffracEVA v.4.2 software provided by Bruker (Bruker, Berlin, Germany). The use of this program code is widely known for determining parameters, and the refinement occurs through a comparative analysis of experimental diffraction patterns with the PDF-2 database, with card values and the subsequent refinement of the parameters by approximation and fitting using mathematical functions built into this program code.

Tests of samples for mechanical stress resistance were carried out using the method of indentation at a pressure on a ceramic sample using a Vickers pyramid indenter with a constant load of 500 N. After the indentation, the shape and size of the indenters were studied to determine the hardness and crack resistance of ceramics, alongside ascertaining the dynamics of changes in these values as a function of the concentration of the Nb_2O_5 dopant and phase composition.

The frequency dependences of the permittivity and dielectric loss tangent of the synthesized ceramics were gauged using a HIOKI IM3533-01 RLC meter in the frequency range 100 Hz–200 kHz. Silver paste was used for the contact electrodes, and was applied on both sides of the tablet to form a flat capacitor. The resulting frequency dependences of the electric capacitance were recalculated into the permittivity. All frequency dependences were measured at room temperature.

3. Results and Discussion

Figure 1 reveals the results of X-ray phase analysis of the studied ferroelectric ceramics of calcium titanate doped with niobium oxide (Nb_2O_5) obtained at various concentrations of Nb_2O_5, which varied from 0.05 to 0.25 mol. The samples were synthesized using the method of mechanochemical synthesis with subsequent thermal annealing of the powders at a temperature of 1300 °C. The dynamics of the presented changes in the obtained X-ray diffraction patterns shows that, with an elevation in the dopant concentration above 0.15 mol, new diffraction reflections appear, which indicates phase transformations associated with structural substitution. Upon analyzing the diffraction patterns acquired from undoped ferroelectric ceramics, it was observed that the diffraction reflection positions align with those typical of the orthorhombic $CaTiO_3$ phase of the Pbnm(62) spatial syngony.

Moreover, the analysis of the ratio of the areas of diffraction reflections with a halo, which is characteristic of background radiation, makes it possible to determine the crystallinity degree, which was more than 86%.
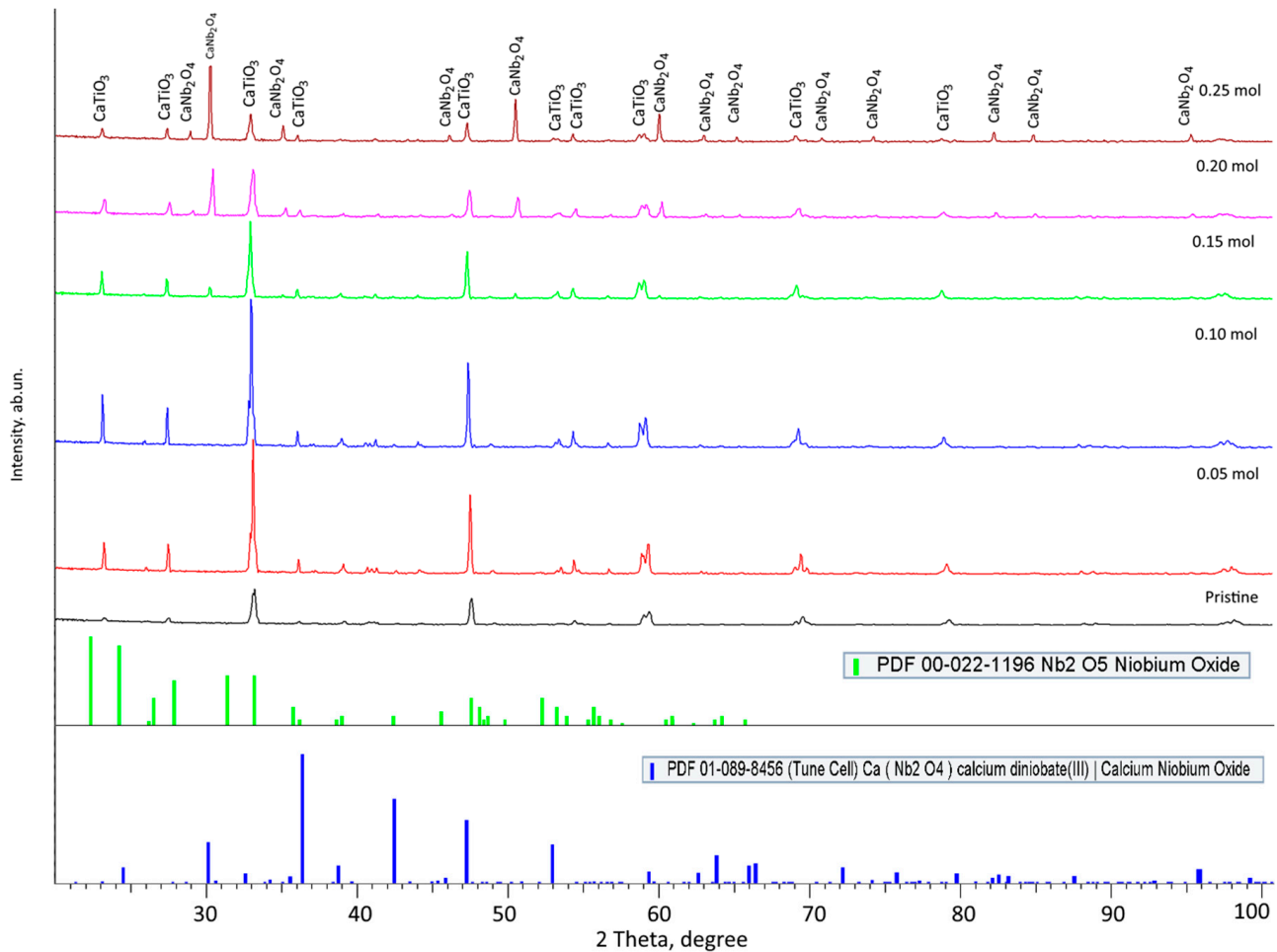

Figure 1. Data of X-ray phase analysis of ferroelectric ceramics of calcium titanate doped with Nb_2O_5. (The X-ray diffraction patterns are supplemented with bar charts for the Nb_2O_5 and $CaNb_2O_4$ phases, which are presented to determine the position of these phases on the samples under study.).

Based on the X-ray phase analysis results provided, when the Nb_2O_5 dopant concentrations ranged from 0.05 to 0.10 mol, the primary structural alterations pertained to the structural ordering of the samples, expressed as a change in the crystallinity degree from 86 to 88–89%. Moreover, the formation of new diffraction reflections with an increase in the Nb_2O_5 concentration from 0.05 mol to 0.10 mol was not established, which indicates that at low contents of the niobium oxide dopant, the processes associated with the emergence of substitution or interstitial phases were not established. However, the established alterations in the crystal lattice parameters with a change in the concentration of the Nb_2O_5 dopant could be due to both the effects of thermal expansion of the crystal lattice and the partial replacement of calcium or titanium ions by niobium ions at the lattice sites. An analysis of the ionic radii for Nb (69 pm), Ca (99 pm), and Ti (68 pm), taking into account changes in the crystal lattice parameters, indicated that such a substitution is possible, taking into account the observed structural changes. The modification in crystal lattice parameters could be further clarified by the increase in niobium concentration within the ceramic composition. Niobium was introduced into interstitial spaces and occupied vacant positions in the structure, which originated from the process of mechanochemical grinding. In this case, grinding led to the emergence of numerous vacancies and structural distortions, which

relaxed under the action of thermal annealing, and vacancies could be filled by introduced dopants, which in turn resulted in a change in the crystal lattice parameters.

At the Nb_2O_5 dopant concentration of 0.15 mol, X-ray diffraction patterns showed the emergence of diffraction reflections typical for the $CaNb_2O_4$ orthorhombic phase of the Pbcm(57) spatial system. The formation of this phase is due to the effect of thermal annealing at temperatures above 1100 °C, at which point a similar phase crystallized in the orthorhombic space group Pbcm with the formation of aligned edges of NbO_6 trigonal prisms, in which Ca^{2+} ions were located in the interlayer space of the trigonal prism. The concentration of this phase was more than 16%.

A further Nb_2O_5 dopant concentration growth to 0.20–0.25 mol resulted in an increase in the content of the contribution of the $CaNb_2O_4$ orthorhombic phase to 29 and 36%, respectively, and the dynamics of fluctuations in the parameters of the crystal lattice and its volume indicated structural ordering and densification of this phase with an increase in its content in the ceramic composition.

The overall pattern in the shift of the phase composition of ferroelectric ceramics as the Nb_2O_5 dopant concentration increases can be characterized by the following sequence of structural-phase transformations: $CaTiO_3 \xrightarrow{0.05-0.10 \text{ mol}}$ structural ordering of the $CaTiO_3$ $\xrightarrow{0.15-0.25 \text{ mol}}$ phase formation of two-phase $CaNb_2O_4/CaTiO_3$ ceramics.

Based on the X-ray phase analysis data acquired, the dependence of the change in the phase composition and the phase ratio while varying the concentration of the Nb_2O_5 dopant in the composition of ferroelectric ceramics was plotted. This dependence is shown in Figure 2. The assessment of the contributions of each phase was carried out by estimating the values of the areas of diffraction reflections established for each phase, followed by calculating the weight contribution using the following Formula (1).

$$V_{\text{admixture}} = \frac{RI_{\text{phase}}}{I_{\text{admixture}} + RI_{phase}} \tag{1}$$

where I_{phase} is the intensity of the main phase, and $I_{admixture}$ is the intensity of the impurity phase, $R = 1.45$.
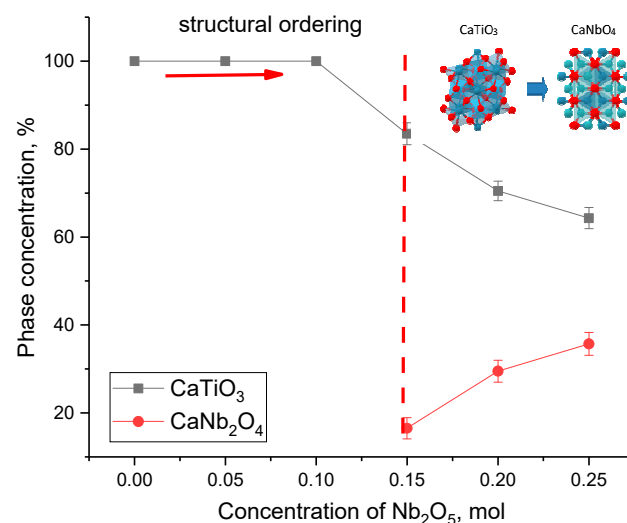

Figure 2. Dependence of the phase composition alteration on the Nb_2O_5 dopant concentration in the composition of ceramics (The inset shows an example of the structural transformation $CaTiO_3 \rightarrow CaNb_2O_4$ upon substitution of niobium ions for titanium ions with the preservation of the orthorhombic motif of the crystal lattice).

The overall view of the presented dependence of the change in the phase composition indicates a two-stage process of variations linked to a fluctuation in the Nb_2O_5 dopant concentration in the ceramics' composition, which consisted of the processes of

structural ordering of the orthorhombic $CaTiO_3$ phase with an increase in the concentration of the Nb_2O_5 dopant from 0.05 to 0.10 mol, as well as the subsequent formation of $CaNb_2O_4/CaTiO_3$ two-phase ceramics, with a growth in the concentration of the $CaNb_2O_4$ orthorhombic phase from 16 to 36 wt. %. In this case, the formation of the $CaNb_2O_4$ phase may be due to the partial replacement of titanium ions by niobium ions in the composition of trigonal prisms, followed by the crystal-structure rearrangement (see inset in Figure 2).

Based on the obtained X-ray diffraction data, the parameters of the crystal lattice and its volume were determined for all observed phases as a function of the variation of the dopant concentration and the observed phase transformations. The data are presented in Table 1.

Table 1. Lattice parameter data.

Phase	Concentration of Nb_2O_5, Mol					
	0.0	0.05	0.10	0.15	0.20	0.25
$CaTiO_3$	a = 5.3672 ± 0.0016 Å, b = 5.4022 ± 0.0013 Å, c = 7.6345 ± 0.0018 Å, V = 221.36 Å^3	a = 5.3681 ± 0.0015 Å, b = 5.4031 ± 0.0016 Å, c = 7.6314 ± 0.0013 Å, V = 221.35 Å^3	a = 5.3775 ± 0.0013 Å, b = 5.4207 ± 0.0018 Å, c = 7.6650 ± 0.0015 Å, V = 223.43 Å^3	a = 5.3765 ± 0.0018 Å, b = 5.4247 ± 0.0014 Å, c = 7.6756 ± 0.0019 Å, V = 223.87 Å^3	a = 5.3744 ± 0.0021 Å, b = 5.4203 ± 0.0019 Å, c = 7.6709 ± 0.0014 Å, V = 223.46 Å^3	a = 5.3754 ± 0.0016 Å, b = 5.4299 ± 0.0012 Å, c = 7.6634 ± 0.0016 Å, V = 223.68 Å^3
$CaNb_2O_4$	-	-	-	a = 5.0609 ± 0.0012 Å, b = 11.9297 ± 0.0015 Å, c = 5.8541 ± 0.0012 Å, V = 353.44 Å^3	a = 5.0481 ± 0.0016 Å, b = 11.8665 ± 0.0013 Å, c = 5.8185 ± 0.0016 Å, V = 348.54 Å^3	a = 5.0421 ± 0.0016 Å, b = 11.8554 ± 0.0014 Å, c = 5.8278 ± 0.0013 Å, V = 348.36 Å^3

Moreover, a rise in the $CaNb_2O_4$ phase in the composition of ceramics with a variation in the dopant concentration led to a decrease in the size of the crystallites, the alteration of which is associated with recrystallization processes and phase transformations caused by structural transformations. It should also be noted that a shift in the phase composition due to the formation of the $CaNb_2O_4$ phase, in addition to affecting the change in the size of crystallites, also affects the change in the structural parameters and the degree of structural ordering. Figure 3 shows the data on changes in the crystallinity degree, reflecting structural ordering alterations in the composition of ceramics with varying concentrations of the Nb_2O_5 dopant.

As can be seen from the data presented, the change in crystallinity exhibited a significant correlation with the dopant concentration, and as a result of the processes, phase transformations that occurred at high concentrations of Nb_2O_5. In the case of an increase in the dopant concentration to 0.05–0.10 mol, an increase in the degree of crystallinity was observed, which is characteristic of the ordering of the crystal structure as a result of the removal of deformation structural distortions [33,34]. The term "structural ordering" in this work means the determination of the ratio of the ordered crystalline phase and disordered deformed inclusions, the presence of which is linked to deformation stresses leading to distortion of the $CaTiO_3$ crystal structure, and the presence of vacancy and point defects in the crystal lattice. An increase or decrease in the structural ordering degree (crystallinity degree) is caused by the processes of changes in the crystal structure of ceramics depending on several factors, including those associated with the formation of a new phase at high dopant concentrations. It should be noted that, at low dopant concentrations (less than 0.15 mol), it is not possible to determine the presence of new phases (their concentration) using X-ray diffraction. At the same time, the data on the crystallinity degree of the undoped sample indicate that the addition of the Nb_2O_5 dopant accelerated the processes

of thermal relaxation of deformation structural distortions, since the crystallinity degree during annealing of the undoped sample was lower than for samples with different dopant concentrations. In the case of phase transformations associated with the formation of the $CaNb_2O_4$ phase in the composition of ceramics, a decrease in the degree of crystallinity was observed, which is due to the processes of deformation distortion of the structure due to the formation of interboundary effects in the composition of the ceramics. As an interboundary effect, the presence of two phases in the structure is implied here, which are presented in the form of grains having a different structure and shape. In this case, when the grains of different phases are close to each other, the so-called interboundary effect or interfacial effect may occur, leading to the creation of additional deformation distortions in the crystal structure, reducing the structural ordering degree (crystallinity degree).
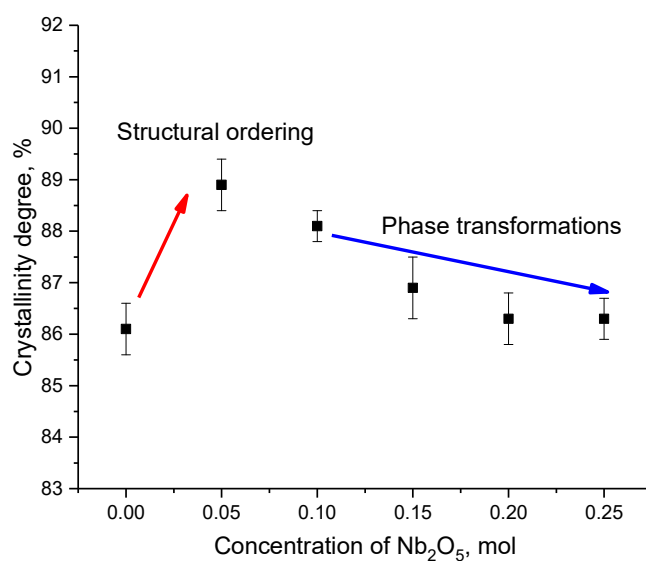

Figure 3. Results of the crystallinity degree variation depending on the Nb_2O_5 dopant concentration.

Figure 4 demonstrates the results of alterations in the density of the studied ceramics depending on the Nb_2O_5 dopant variation in the composition of ceramics, as well as reflecting the relationship between alterations in the density of ceramics and their phase compositions. As is evident from the data presented, the density change led to a clear increase at the Nb_2O_5 dopant concentration of 0.15 mol, followed by a more pronounced increase than at lower dopant concentrations. This increase and subsequent growth is primarily due to the fact that, at dopant concentrations of 0.15 mol and higher, the $CaNb_2O_4$ phase was formed in the ceramic structure, the density of which in the ordered state was 5.3 g/cm^3, while the density of $CaTiO_3$ was 3.8 g/cm^3. In turn, the change in density with a variation in concentrations of 0.05–0.10 mol was associated with a change in the structural ordering degree, alongside a decrease in the crystal lattice volume, indicating a decline in deformation distortions and stresses in the structure of ceramics. This change is associated primarily with the processes of phase formation and structural ordering during the thermal annealing of ceramics. An increase in the $CaNb_2O_4$ phase contribution leads to more pronounced changes in density, which is associated with the formation of denser ceramics. In this case, when the ratio of the $CaNb_2O_4/CaTiO_3$ phases is close to the ratio of 30/70, the density increases by 18%, which indicates sufficient compaction of the ceramics with a change in the phase composition, which can subsequently lead to a change in the strength and dielectric characteristics.
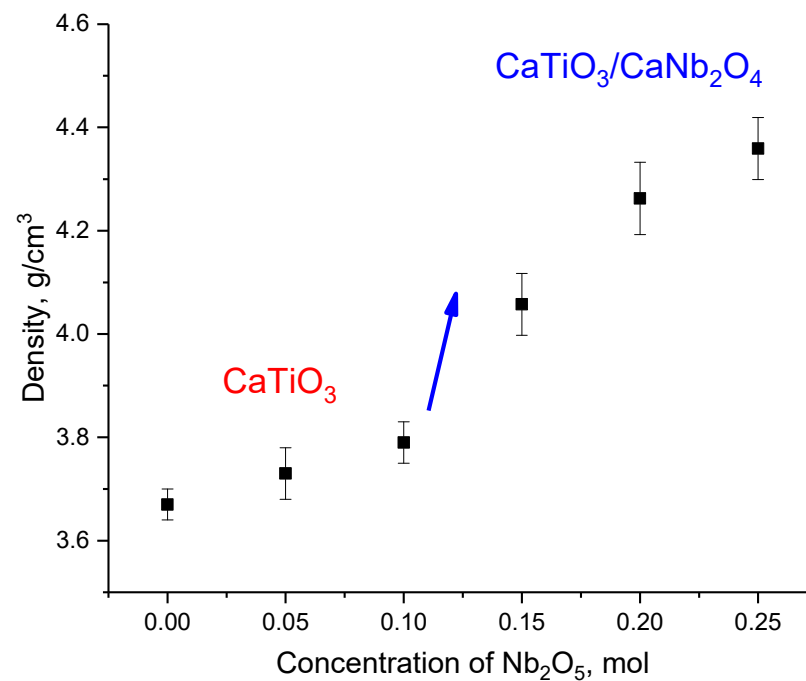
Figure 4. Graph of the dependence of the change in the density of ceramics with a variation in the Nb_2O_5 dopant in the composition.

Figure 5 demonstrates the results of the measurements of morphological features performed using scanning electron microscopy, in the form of SEM images taken at one magnification in order to display alterations in the shape and size of ceramic grains. As is evident from the data on changes in the morphological features of grains and their sizes, a direct dependence of the influence of dopant variation on the morphology of the obtained structures can be traced. At low concentrations of the Nb_2O_5 dopant (0.05–0.10 mol) in the composition of ceramics, the main changes are associated with coarsening of grains, and the formation of developed dendritic agglomerates consisting of grains of different sizes. The formation of dendritic agglomerates is due to the sintering of grains with each other, resulting in the formation of agglomerates having a rather complex geometric shape. In this case, "dendritic agglomerates" means the presence of structures in the form of large grains surrounded by smaller grains in the form of branched outgrowths, the formation of which is due to sintering processes during thermal annealing. In the case of high concentrations, the formation of a more ordered structure of ceramics was observed, consisting of grains of approximately equal sizes, combined with each other. As a rule, these dendrites are a combination of two three large grains larger than 500 nm, surrounded by smaller spherical grains in the form of processes. Moreover, in the case of varying the Nb_2O_5 concentration, in addition to the coarsening of grains, an elevation in the degree of their homogeneity in size (i.e., the number of grains of the same size) was also observed, which implies that the addition of a dopant results in the initialization of the structural-phase ordering processes, accompanied by the coarsening of grains and their agglomerations into dendrites. In the case when, according to the data of X-ray phase analysis, the appearance of the $CaNb_2O_4$ phase was observed in the composition of the ceramics, the formation of grains of a feather-like shape was observed in the structure of the ceramics, which may be associated with the formation of new inclusions in the composition. The sizes of these grains had significant differences to large agglomerates, and these grains were formed in the form of growths and inclusions near the boundaries of larger grains in agglomerates. When it came to an increase in the Nb_2O_5 dopant concentration to 0.20–0.25 mol, the formation of close-packed grains was observed, in which finer $CaNb_2O_4$ grains were located in the interboundary space.
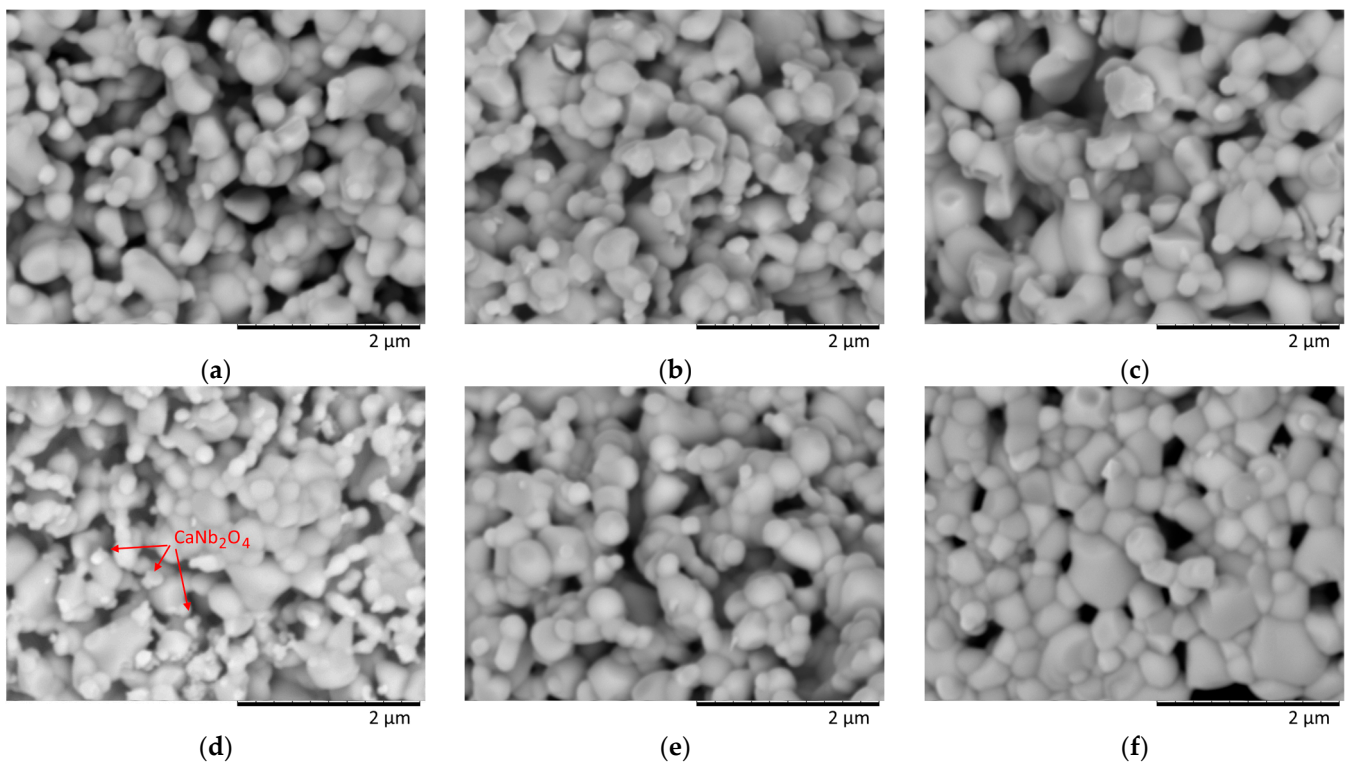
Figure 5. Images of ceramic surface morphology with varying Nb_2O_5 dopant concentration: (**a**) pristine; (**b**) 0.05 mol; (**c**) 0.10 mol; (**d**) 0.15 mol; (**e**) 0.20 mol; (**f**) 0.25 mol.

Thus, by analyzing the changes in the morphological features of the synthesized ceramics depending on the Nb_2O_5 dopant concentration, it can be concluded that at low dopant concentrations (0.05–0.15 mol), the main changes are associated with grain enlargement, with the subsequent formation of dendritic formations. Regarding high concentrations, a close-packed structure is formed with the inclusion of $CaNb_2O_4$ grains in the interboundary space.

One of the important parameters of the use of ceramics in various practical applications, in particular, their use as fuel cells or anode materials, is their resistance to mechanical stress. At the same time, in most cases, for ferroelectric ceramics, the hardness values are rather low, which leads to their rapid embrittlement and destruction under external influences, including mechanical pressures. The most common methods for increasing the resistance of ferroelectric ceramics to external influences and increasing the strength characteristics are either a reduction in the grain size, which results in an elevation in the dislocation density, or the creation of interfacial boundaries due to a variation in the phase composition of the ceramics by doping. In the first case, the effect of dislocation hardening can play both a positive role associated with an increase in resistance to cracking and crack formation due to the presence of a high density of dislocations that prevent the propagation of microcracks, and a negative role associated with supersaturation of the ceramic structure with dislocations, which can result in embrittlement and a decrease in its impact strength and elasticity. Doping, in turn, leading to the emergence of impurity phases results in the formation of additional interfacial boundaries, which creates obstacles for the propagation of cracks, and also increases resistance to external influences. It is well known that the formation of impurity inclusions in the structure results in an increase in its resistance to external influences and the formation of microcracks under loads. Also, an important factor in doping, which can affect the increase in stability, is represented by density, the change in which is directly related to the phase-composition alteration during the formation of impurity phases.

Figure 6 reveals the results of fluctuations in the hardness and crack resistance of ferroelectric ceramics depending on the concentration of the dopant, reflecting the effects of hardening with variations in the phase composition and density of the ceramics.
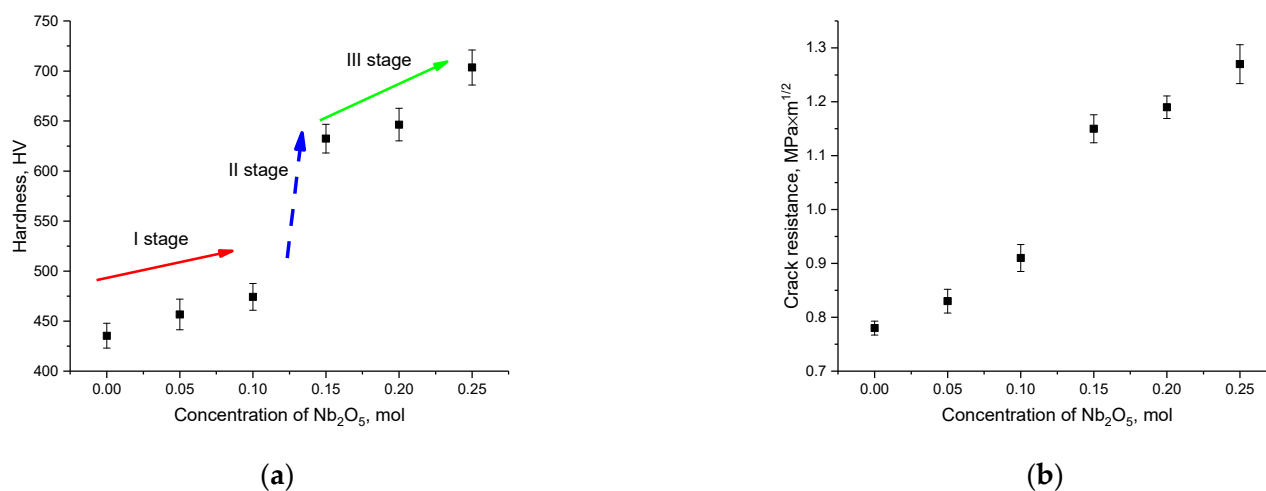

(**a**)

(**b**)

Figure 6. (**a**) Results of variation in hardness as a function of the concentration of the Nb_2O_5 dopant (arrows indicate the main stages associated with changes in the strength characteristics of ferroelectric ceramics); (**b**) results of the evaluation of the crack resistance of ceramics with a variation in the Nb_2O_5 dopant concentration.

As is evident from the data presented in Figure 6a, the overall view of alterations in hardness values can be divided into three main stages associated with a different trend of increasing hardness. The first stage is characterized by small changes in hardness (no more than 1–2%), which occur when adding Nb_2O_5 dopant in a concentration of 0.05–0.10 mol. Such a small variation in hardness, as a result of the strengthening effect, is primarily due to the absence of phase transformation processes at these concentrations, which does not result in the creation of interfacial boundaries in the composition of ceramics. A slight increase in hardness values in this range is due to a fluctuation in the structural ordering degree caused by the thermal annealing of point defects, and a decrease in porosity, as evidenced by a variation in the density of ceramics. The second stage is characterized by a sharp increase in hardness from 475 HV to 630 HV, and the hardening effect was more than 30%. This effect is due to the formation of the $CaNb_2O_4$ phase in the composition of ceramics, which leads to the formation of interfacial boundaries, as well as an increase in the density of ceramics [35,36]. At the same time, for the third stage, which is typical for dopant concentrations of 0.20–0.25 mol, the strengthening efficiency, in comparison with the hardness values of the sample obtained at a dopant concentration of 0.15 mol, is no more than 10%, and the trend of hardness change with a rise in the dopant concentration is characteristic of the trend of the first stage. The explanation for such small changes in the values of hardness and hardening with a growth in the concentration of the $CaNb_2O_4$ phase, and, as a consequence, a change in the number of grain boundaries, could be the fact that a decrease in the degree of structural ordering was observed during the formation of a large amount of this impurity phase. The decrease in the structural ordering degree was due to the effects of phase formation processes, which lead to the appearance of structural distortions and deformations in ceramics, which affect the change in the crystal lattice perfection. In this case, an increase in the number of interfacial boundaries and their effect on hardening is partially offset by the effect of structural disorder associated with the formation of a high concentration of the $CaNb_2O_4$ phase.

The fracture resistance results show similar trend changes (see Figure 6b) as a function of Nb_2O_5 dopant concentration and changes in the phase composition of ferroelectric ceramics as hardness values. At the same time, the $CaNb_2O_4$ phase formation at a dopant concentration of 0.15 mol results in a crack resistance growth by only 25%, while hardening

(i.e., a change in hardness) was more than 30%. This difference may be due to the fact that during the formation of the $CaNb_2O_4$ impurity phase, the resistance to external pressure becomes greater than to the formation of cracks.

The results of measurements of the dielectric constant in the frequency range 100 Hz–200 kHz are shown in Figure 7a. As can be seen from the given frequency dispersion curves, the permittivity in the measured frequency range was not found. In many works, the pronounced frequency dependence of ε' in the low-frequency region in perovskite ceramics is associated with the Maxwell–Wagner polarization [37]. In the case of the samples synthesized in this work, this polarization mechanism was not observed even in two-phase ceramics, which may be due to the effect of pores in the microstructure, which were detected in SEM micrographs. The appearance of a high dielectric constant in perovskite crystal structures is associated with a slight distortion of the sublattices upon the introduction of ions with a large radius (Ca^{2+}, Ba^{2+}, Sr^{2+}. Bi^{2+}). The values of ε' in ceramics of $BaTiO_3$—ZrO_2—$CaTiO_3$ solid solutions have been reported in the range of 1000–2900 [38]. Due to the influence of pores in the studied samples, the values of ε' are significantly reduced. In addition, a decrease in the value of the dielectric constant is observed upon the introduction of a dopant, starting from a concentration of 0.05 mol. To establish the reasons for this behavior of the samples, it is necessary to consider the formation of large values of ε' in perovskite polycrystals. A slight distortion of the crystal lattice by the ion creates a pronounced charge redistribution in the structure, which in turn creates dipoles with a large moment. The introduction of a rare-earth element into the perovskite lattice changes the dipole moment. The dielectric constant of an oxide crystal is the sum of the contributions of ionic polarization and electron polarization, and also depends on the effective charge of the crystal lattice polyhedron, the contribution of transverse optical phonons, and the polarizability of electrons surrounding the ions [39]. The incorporation of rare-earth atoms of the Nd, Sm, and Nb types can disrupt the long-range order [40] and also change the effective charge of polyhedra in the crystal [41]. It has been established using X-ray diffraction methods that at a dopant concentration of 0.15 mol, the cations in $CaTiO_3$ are replaced by Nb ions, which leads to the above-described case. The minimum value for the sample with 0.10 mol could be related to the large size of the ceramic grains, which could lead to their less-dense packing and the formation of pores with a larger radius. In addition, an important contribution to the permittivity is made by the grains of the second phase of $CuNb_2O_4$, the value of which is lower than that for $CaTiO_3$ (~180). In [41], it was reported that at room temperature in Cu-Nb perovskite, the value of ε' is 18. In that case, the formation of this phase reduces the value of the permittivity with increasing dopant concentration, which is observed in the frequency dependences of $\varepsilon'(f)$. It can be argued that, according to the results of the SEM analysis, all the obtained samples have a pronounced porosity, which indicates the greatest contribution to the decrease in the dielectric constant of fluctuations in the phase composition or structural characteristics of the crystal, which in turn affects the polarization.

The increased values of dielectric losses in the low-frequency region in the tan δ frequency spectra (Figure 7b) are associated with the ceramic structure: the presence of grain boundaries, the presence of perovskite $CaTiO_3/CaNb_2O_4$ interfaces, and the presence of pores. It can be noted that, as the dopant concentration increases, the dielectric loss, in contrast to the dielectric permittivity, increases. In general, in the frequency range of 1–200 kHz, the dielectric loss is < 0.01, which characterizes the obtained ceramic as a dielectric with a high-quality factor. The increase in dielectric losses can be associated with the multivalence of Nb ions, which forces the valence of Ti ions to change. A change in the $Ti^{4+} \rightarrow Ti^{3+}$ valence can increase the value of tan δ in Ti-containing oxide ceramics [41].
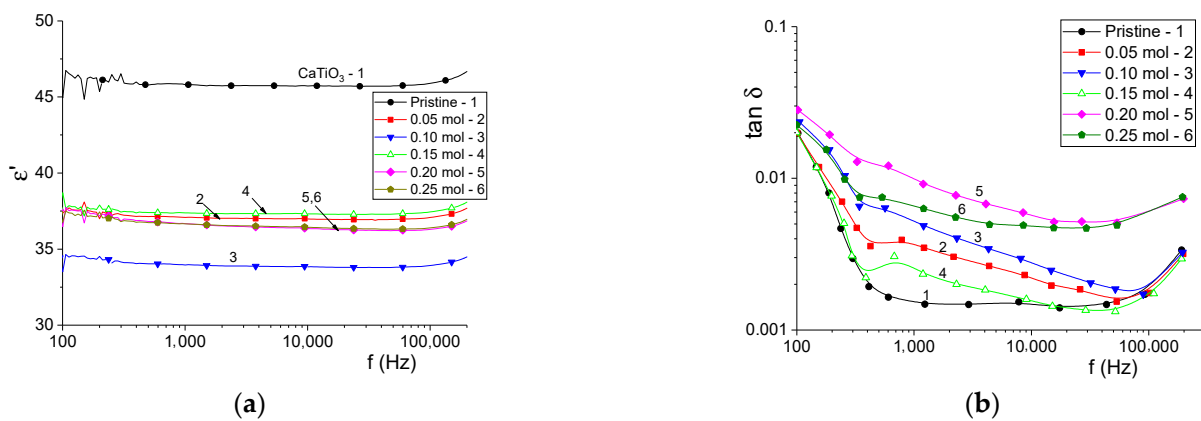
Figure 7. Frequency dependence of permittivity (**a**) and dielectric loss tangent (**b**) for synthesized ceramics at room temperature.

One of the important parameters characterizing the resistance of ferroelectric ceramics to external influences is their thermal stability to prolonged heating, which can lead to thermal expansion (linear or volumetric), which in turn can adversely affect not only the alteration in the structural characteristics of ceramics, but also the preservation of mechanical properties. Figure 8 demonstrates the results of changing the value of the volume expansion coefficient ($\beta_V(T)$), which reflects changes in the crystal lattice volume as a result of long-term endurance tests. Formula (2) was used to calculate the value of $\beta_V(T)$:

$$\beta_V(T) = \frac{1}{V_{initial}} \frac{\Delta V}{\Delta T}, \tag{2}$$

where $V_{initial}$ is the crystal lattice volume before the life tests; V_h is the volume of the crystal lattice after a certain time of the life tests; $\Delta V = (V_{initial} - V_h)$; $\Delta T = 873$ K. Life tests to determine the value of $\beta_V(T)$ were executed in a muffle furnace at a temperature of 873 K, which is typical for the operating temperature of anode materials in solid oxide fuel cells. The choice of time frames for estimating the change in the value of $\beta_V(T)$ was determined by the operating modes.
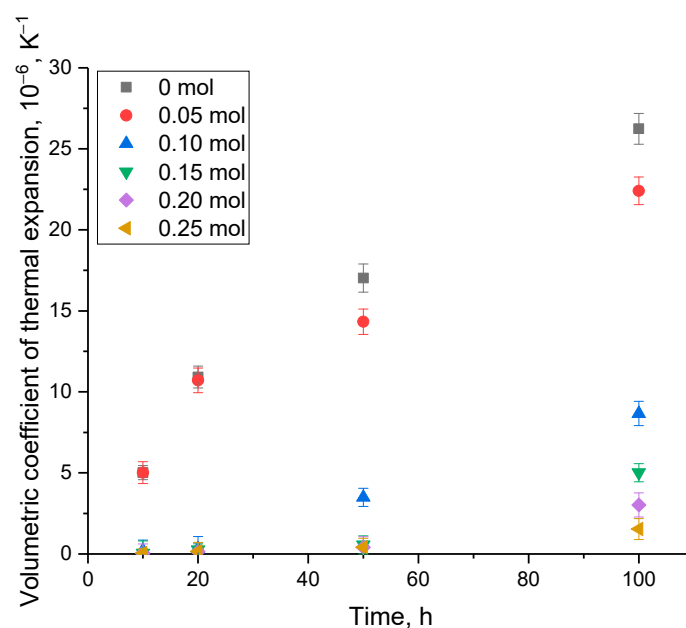

Figure 8. Results of evaluation of the variation in the value of $\beta_V(T)$ for the studied ceramics depending on the test time.

As is evident from the presented data, changes in the value of $\beta_V(T)$ depending on the time of thermal exposure and changes for undoped ceramics, as well as those doped with a concentration of 0.05 mol, were observed already after 10 h of testing, which indicates a rather low resistance of ceramics to the thermal expansion of the crystal structure during operation. At the same time, for these samples, the increase in $\beta_V(T)$ after 100 h of testing in comparison with the value after 10 h of testing was more than five times. Such a change in the value of $\beta_V(T)$ for undoped ceramics indicates a high rate of structural degradation associated with the broadening of the lattice volume and its swelling as a result of external temperature factors. In the case of doped ceramics with a concentration of more than 0.10 mol, for which the formation of the $CaNb_2O_4$ phase in the structure was observed, the main changes were observed after 50 h of life tests, while a shorter thermal exposure time led to changes in the $\beta_V(T)$ value of less than 0.1%. It should also be noted that an elevation in the $CaNb_2O_4$ phase content results in smaller changes in the value of $\beta_V(T)$ during long-term tests, and at times of less than 50 h, changes in the value of $\beta_V(T)$ with variations in the concentration of the dopant are practically not observed. At the same time, the maximum value of changes in $\beta_V(T)$ for two-phase ceramics is 5–7-times less than the same value for undoped single-phase ceramics. One of the explanations for the effect of a decrease in the degradation rate (the magnitude of the change in $\beta_V(T)$ during temporary life tests) for two-phase ceramics could be the factor of the presence of interphase boundaries, as well as partial replacement of calcium or titanium by niobium ions at the nodes of the crystal lattice, which leads to an increase in the resistance of the crystal lattice to swelling due to thermal expansion. At the same time, from the presented data, the effect of an increase in the weight contribution of the $CaNb_2O_4$ phase on a decrease in the value of $\beta_V(T)$ is clearly seen, which leads to the fact that at a ratio of $CaNb_2O_4/CaTiO_3$ phases close to the ratio of 30/70, the value of $\beta_V(T)$ after 100 h of testing was an order of magnitude lower than for the single-phase ceramics. Thermal expansion of the crystal structure as a result of external influences during life tests can also affect the stability of the strength properties (hardness and crack resistance) of ceramics. Figure 9 shows the results of an assessment of the change in strength characteristics after 100 h of thermal exposure, reflecting the alteration in the resistance of ceramics to external influences during thermal heating for a long time, comparable both with the effect of operation and the effect of high-temperature aging.
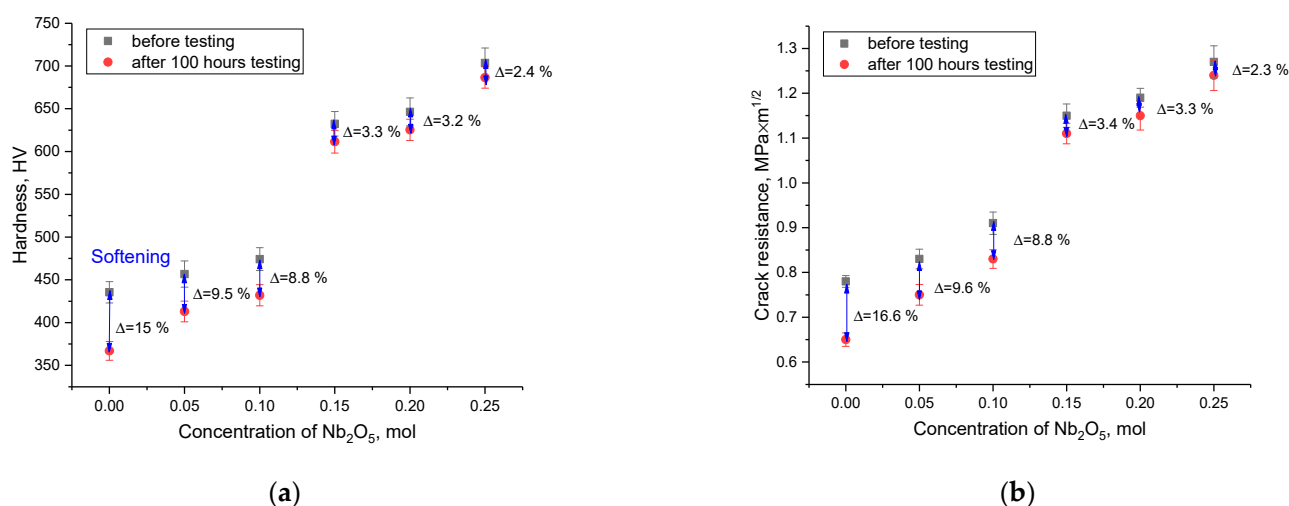

Figure 9. Results of changes in the values of hardness (**a**) and crack resistance (**b**) of ceramics before and after life tests for thermal stability.

An examination of the shifts in hardness and crack resistance values of ceramics after 100 h of thermal-stability life testing, in comparison to the initial values, illustrates a clear connection between the hardening effect and the ceramics' phase composition. In

the case of structurally ordered ceramics obtained at an Nb_2O_5 dopant concentration of 0.05–0.10 mol, the decrease in strength characteristics was no more than 10%, while for the original sample, the deterioration in hardness and crack resistance was more than 15% after 100 h of life tests. Regarding two-phase ceramics, the reduction in strength characteristics after 100 h of testing was no more than 2.2–3%, which, as in the case with a change in the $\beta_V(T)$ value, indicates a positive effect of the presence of the $CaNb_2O_4$ phase on the strengthening of ceramics and a rise in their resistance and thermal stability.

4. Conclusions

This paper revealed the results of evaluating the effect of phase transformations associated with the emergence of impurity inclusions in the form of $CaNb_2O_4$, in the structure of ferroelectric ceramics based on calcium titanate, on the alteration in dielectric and strength properties. The synthesis of ceramics was carried out through the mechanochemical mixing of the initial components at various concentrations of the Nb_2O_5 dopant, followed by thermal sintering and pressing of samples into ceramics. According to the data of X-ray phase analysis, it was found that an increase in the Nb_2O_5 dopant concentration led to the formation of $CaNb_2O_4$ phase inclusions in the ceramic structure, the maximum content of which was no more than 30% at the Nb_2O_5 concentration of 0.25 mol. An analysis of the morphological features of the synthesized ceramics demonstrated that the addition of Nb_2O_5 leads to the formation of larger structures, and in the case of the formation of the $CaNb_2O_4$ phase in the structure, ceramics are close-packed agglomerations of grains, the interboundary space in which is occupied by $CaNb_2O_4$ grains. An analysis of the strength characteristics as a function of changes in the phase composition showed a direct relationship between hardening and crack-resistance growth during the formation of the two-phase ceramics.

Thus, the experiments performed indicated a positive effect of the Nb_2O_5 dopant on the change in properties, and an increase in the resistance to thermal aging during life tests of ferroelectric ceramics based on calcium titanate.

Author Contributions: Conceptualization, M.V.Z., A.L.K., G.Z.M., R.I.S., D.B.B. and I.Z.Z.; methodology M.V.Z., A.L.K., G.Z.M., R.I.S., D.B.B. and I.Z.Z.; formal analysis, M.V.Z., A.L.K., G.Z.M., R.I.S., D.B.B. and I.Z.Z.; investigation, M.V.Z. and A.L.K.; resources, M.V.Z., A.L.K., G.Z.M., R.I.S., D.B.B. and I.Z.Z.; writing—original draft preparation, review, and editing, M.V.Z., A.L.K., G.Z.M., R.I.S., D.B.B. and I.Z.Z.; visualization, M.V.Z., D.B.B. and A.L.K.; supervision, M.V.Z. and A.L.K. All authors have read and agreed to the published version of the manuscript.

Data Availability Statement: Not applicable.

Conflicts of Interest: The authors declare that they have no conflicts of interest.

References

1. Khan, I.; Khan, A.; Khan, M.M.A.; Khan, S.; Verpoort, F.; Umar, A. (Eds.) *Hybrid Perovskite Composite Materials: Design to Applications*; Woodhead Publishing: Thurston, UK, 2020.
2. Chen, M.; Xiong, Q.; Liu, Z.; Qiu, K.; Xiao, X. Synthesis and photocatalytic activity of Na+ co-doped $CaTiO_3$: Eu3+ photocatalysts for methylene blue degradation. *Ceram. Int.* **2020**, *46*, 12111–12119. [CrossRef]
3. Gazda, M.; Jasinski, P.; Kusz, B.; Bochentyn, B.; Gdula-Kasica, K.; Lendze, T.; Molin, S. Perovskites in solid oxide fuel cells. *Solid State Phenom.* **2012**, *183*, 65–70.
4. Muñoz-García, A.B.; Ritzmann, A.M.; Pavone, M.; Keith, J.A.; Carter, E.A. Oxygen transport in perovskite-type solid oxide fuel cell materials: Insights from quantum mechanics. *Acc. Chem. Res.* **2014**, *47*, 3340–3348. [CrossRef] [PubMed]
5. Skinner, S.J. Recent advances in Perovskite-type materials for solid oxide fuel cell cathodes. *Int. J. Inorg. Mater.* **2001**, *3*, 113–121. [CrossRef]
6. Sunarso, J.; Hashim, S.S.; Zhu, N.; Zhou, W. Perovskite oxides applications in high temperature oxygen separation, solid oxide fuel cell and membrane reactor: A review. *Prog. Energy Combust. Sci.* **2017**, *61*, 57–77. [CrossRef]
7. Jiang, S.P. Development of lanthanum strontium cobalt ferrite perovskite electrodes of solid oxide fuel cells-A review. *Int. J. Hydrog. Energy* **2019**, *44*, 7448–7493. [CrossRef]

8. Žužić, A.; Ressler, A.; Macan, J. Perovskite oxides as active materials in novel alternatives to well-known technologies: A review. *Ceram. Int.* **2022**, *48*, 27240–27261. [CrossRef]

9. Monama, G.R.; Ramohlola, K.E.; Iwuoha, E.I.; Modibane, K.D. Progress on perovskite materials for energy application. *Res. Chem.* **2022**, *4*, 100321. [CrossRef]

10. Suzuki, K.; Kouchi, Y.; Hirota, T.; Kato, H.; Namioka, T.; Ito, H.; Hong, H.-J.; Yashiro, K.; Kawada, T.; Okai, K.; et al. Study of $CaTiO_3$ based ionic conductors for lightweight SOFCs. *ECS Trans.* **2019**, *91*, 1217–1222. [CrossRef]

11. Ji, Q.; Bi, L.; Zhang, J.; Cao, H.; Zhao, X.S. The role of oxygen vacancies of ABO_3 perovskite oxides in the oxygen reduction reaction. *Energy Environ. Sci.* **2020**, *13*, 1408–1428. [CrossRef]

12. Sando, D. Strain and orientation engineering in ABO_3 perovskite oxide thin films. *J. Phys. Condens. Matter* **2022**, *34*, 153001. [CrossRef] [PubMed]

13. Souri, M.; Amoli, H.S. Gas sensing mechanisms in ABO_3 perovskite materials at room temperature: A review. *Mater. Sci. Semicond. Process.* **2023**, *156*, 107271. [CrossRef]

14. Kim, H.; Hwang, D.; Kim, Y.; Lee, J. Highly donor-doped (110) layered perovskite materials as novel photocatalysts for overall water splitting. *Chem. Commun.* **1999**, *12*, 1077–1078. [CrossRef]

15. Min, K.; Cho, E. Accelerated discovery of potential ferroelectric perovskite via active learning. *J. Mater. Chem. C* **2020**, *23*, 7866–7872. [CrossRef]

16. Kim, E.; Kim, J.; Min, K. Prediction of dielectric constants of ABO 3-type perovskites using machine learning and first-principles calculations. *Phys. Chem. Chem. Phys.* **2022**, *11*, 7050–7059. [CrossRef]

17. Shen, Q.; Dong, S.; Li, S.; Yang, G.; Pan, X. A review on the catalytic decomposition of NO by perovskite-type oxides. *Catalysts* **2021**, *11*, 622. [CrossRef]

18. Zhu, L.; Ran, R.; Tadé, M.; Wang, W.; Shao, Z. Perovskite materials in energy storage and conversion. *Asia-Pac. J. Chem. Eng.* **2016**, *11*, 338–369. [CrossRef]

19. Mi, J.; Chen, J.; Chen, X.; Liu, X.; Li, J. Recent Status and Developments of Vacancies Modulation in the ABO_3 Perovskites for Catalytic Applications. *Chem. Eur. J.* **2023**, *29*, e202202713. [CrossRef]

20. Pihlatie, M.; Kaiser, A.; Mogensen, M. Mechanical properties of NiO/Ni–YSZ composites depending on temperature, porosity and redox cycling. *J. Eur. Ceram. Soc.* **2009**, *29*, 1657–1664. [CrossRef]

21. Talebi, T.; Sarrafi, M.H.; Haji, M.; Raissi, B.; Maghsoudipour, A. Investigation on microstructures of NiO–YSZ composite and Ni–YSZ cermet for SOFCs. *Int. J. Hydrog. Energy* **2010**, *35*, 9440–9447. [CrossRef]

22. Bao, Y.; Zhang, F. Electronic Engineering of ABO_3 Perovskite Metal Oxides Based on d 0 Electronic-Configuration Metallic Ions toward Photocatalytic Water Splitting under Visible Light. *Small Struct.* **2022**, *3*, 2100226. [CrossRef]

23. Ye, X.; Wang, X.; Liu, Z.; Zhou, B.; Zhou, L.; Deng, H.; Long, Y. Emergent physical properties of perovskite-type oxides prepared under high pressure. *Dalton Trans.* **2022**, *51*, 1745–1753. [CrossRef] [PubMed]

24. Xu, P.; Chang, D.; Lu, T.; Li, L.; Li, M.; Lu, W. Search for ABO_3 type ferroelectric perovskites with targeted multi-properties by machine learning strategies. *J. Chem. Inf. Model.* **2021**, *62*, 5038–5049. [CrossRef] [PubMed]

25. Bhojanaa, K.B.; Soundarya Mary, A.; Shalini Devi, K.S.; Pavithra, N.; Pandikumar, A. Account of Structural, Theoretical, and Photovoltaic Properties of ABO_3 Oxide Perovskites Photoanode-Based Dye-Sensitized Solar Cells. *Sol. RRL* **2022**, *6*, 2100792. [CrossRef]

26. Passi, M.; Pal, B. A review on $CaTiO_3$ photocatalyst: Activity enhancement methods and photocatalytic applications. *Powder Technol.* **2021**, *388*, 274–304. [CrossRef]

27. Navas, D.; Fuentes, S.; Castro-Alvarez, A.; Chavez-Angel, E. Review on sol-gel synthesis of perovskite and oxide nanomaterials. *Gels* **2021**, *7*, 275. [CrossRef] [PubMed]

28. Rizwan, M.; Usman, Z.; Shakil, M.; A Gillani, S.S.; Azeem, S.; Jin, H.B.; Cao, C.; Mehmood, R.F.; Nabi, G.; Asghar, M.A. Electronic and optical behaviour of lanthanum doped $CaTiO_3$ perovskite. *Mater. Res. Express* **2020**, *7*, 015920. [CrossRef]

29. Dereń, P.; Lemański, K. Cross relaxation in $CaTiO_3$ and $LaAlO_3$ perovskite nanocrystals doped with Ho^{3+} ions. *J. Lumin.* **2014**, *154*, 62–67. [CrossRef]

30. Zhou, S.; Luan, X.; Hu, S.; Zhou, X.; He, S.; Wang, X.; Zhang, H.; Chen, X.; Zhou, H. Sintering behavior, phase structure and microwave dielectric properties of CeO_2 added $CaTiO_3$-$SmAlO_3$ ceramics prepared by reaction sintering method. *Ceram. Int.* **2021**, *47*, 3741–3746. [CrossRef]

31. Dou, Z.M.; Wang, G.; Jiang, J.; Zhang, T.J. Effect of Nd_2O_3 on the Microwave Dielectric Properties of 0.67 $CaTiO_3$-0.33 $LaAlO_3$ Ceramics. *Key Eng. Mater.* **2017**, *726*, 215–219.

32. Omran, K.; Mostafa, M.; El-Sadek, M.A.; Hemeda, O.; Ubic, R. Effects of Ca doping on structural and optical properties of PZT nanopowders. *Results Phys.* **2020**, *19*, 103580. [CrossRef]

33. Su, Z.; Tan, J.M.R.; Li, X.; Zeng, X.; Batabyal, S.K.; Wong, L.H. Cation substitution of solution-processed Cu_2ZnSnS_4 thin film solar cell with over 9% efficiency. *Adv. Energy Mater.* **2015**, *5*, 1500682. [CrossRef]

34. Su, C.; Ao, L.; Zhang, Z.; Zhai, Y.; Chen, J.; Tang, Y.; Liu, L.; Fang, L. Crystal structure, Raman spectra and microwave dielectric properties of novel temperature-stable $LiYbSiO4$ ceramics. *Ceram. Int.* **2020**, *46*, 19996–20003. [CrossRef]

35. Thimmappa, S.K.; Golla, B.R.; Prasad, V.B.; Majumdar, B.; Basu, B. Phase stability, hardness and oxidation behaviour of spark plasma sintered ZrB_2-SiC-Si_3N_4 composites. *Ceram. Int.* **2019**, *45*, 9061–9073. [CrossRef]

36. Muir, C.D.S. *(Ca,Zn)Nb_2O_6-Microwave Dielectric Ceramics*; The University of Manchester: Manchester, UK, 2004.

37. Kamba, S.; Bovtun, V.; Petzelt, J.; Rychetsky, I.; Mizaras, R.; Brilingas, A.; Banys, J.; Grigas, J.; Kosec, M. Dielectric dispersion of the relaxor PLZT ceramics in the frequency range 20 Hz–100 THz. *J. Phys. Condens.* **2000**, *12*, 497–519. [CrossRef]

38. Acosta, M.; Novak, N.; Rojas, V.; Patel, S.; Vaish, R.; Koruza, J.; Rossetti, G.A., Jr.; Rödel, J. BaTiO$_3$-based piezoelectrics: Fundamentals, current status, and perspectives. *Appl. Phys. Rev.* **2017**, *4*, 041305. [CrossRef]

39. Danilkevitch, M.I.; Makoed, I.I. Dielectric properties of spinel, garnet and perovskite oxides. *Phys. Status Solidi B* **2000**, *222*, 541–551. [CrossRef]

40. Lemanov, V.V.; Sotnikov, A.V.; Smirnova, E.P.; Weihnacht, M.; Kunze, R. Perovskite CaTiO$_3$ as an incipient ferroelectric. *Solid State Commun.* **1999**, *110*, 611–614. [CrossRef]

41. Zhang, J.; Wang, J.; Gao, D.; Liu, H.; Xie, J.; Hu, W. Enhanced energy storage performances of CaTiO$_3$-based ceramic through A-site Sm3+ doping and A-site vacancy. *J. Eur. Ceram.* **2021**, *41*, 352–359. [CrossRef]